Applied and Computational Mechanics 8 (2014) 115–128

Double pendulum contact problem

J. Špička[a,*], L. Hynčík[a], M. Hajžman[a]

[a]Faculty of Applied Sciences, University of West Bohemia in Pilsen, Univerzitní 8, 306 14 Plzeň, Czech Republic

Received 12 December 2013; received in revised form 28 April 2014

Abstract

The work concerns contact problems focused on biomechanical systems modelled by a multibody approach. The example is modelling of impact between a body and an infrastructure. The paper firstly presents algorithm for minimum distance calculation. An analytical approach using a tangential plain perpendicular to an initial one is applied. Contact force generated during impact is compared by three different continuous force models, namely the Hertz's model, the spring-dashpot model and the non-linear damping model. In order to identify contact parameters of these particular models, the method of numerical optimization is used. Purpose of this method is to find the most corresponding results of numerical simulation to the original experiment. Numerical optimization principle is put upon a bouncing ball example for the purpose of evaluation of desirable contact force parameters. The contact modelling is applied to a double pendulum problem. The equation of motion of the double pendulum system is derived using Lagrange equation of the second kind with multipliers, respecting the contact phenomena. Applications in biomechanical research are hinted at arm gravity motion and a double pendulum impact example.

Keywords: contact, continuous contact model, minimum distance calculation, contact force parameters

1. Introduction

Contact or impact is a very frequent phenomenon that occurs when two or more bodies undergo a collision. A contact problem arises in numerous engineering applications, such as multibody dynamics, robotics, biomechanics and many others. Impact in biomechanical research studies the consequences to the human body impact like a car crash, pedestrian impact, falls and sports injuries or contact in forensic applications. This field motivates engineers and designers to develop better safety systems for people exposed to impact injuries. Virtual human body models start to play an important role in the impact biomechanics. Multibody models can evaluate human body kinematics under external loading quickly. Detailed deformable models can then simulate tissue injuries, however these models spend a lot of computational time. Thus articulated rigid bodies can be sufficient tool for the first approximation and they might predict long duration global human body behaviour in very short time. For such models, contact modelling and contact parameters evaluating are crucial aspects of a successful description.

This work describes double pendulum as a simple articulated rigid body system based on multibody approach, e.g. [10] or [12]. Author uses Lagrange equation with multipliers to evaluate equations of motion. Derivation of an impact algorithm using various contact force models is demonstrated. The solution of contact problems is very complex as is shown e.g. in [8]. The three implemented contact force models are Hertz model, spring-dashpot model and non-linear damping model [5], respectively. This work also presents an algorithm for minimum distance calculation between a body and a plain using analytical approach based on the plain tangential

*Corresponding author. Tel.: +420 377 634 743, e-mail: spicka@ntc.zcu.cz.

to the body. Principle of numerical optimization is applied on a simple mechanics example of a bouncing ball in order to evaluate contact parameters according to a real system. Optimized values of contact force parameters are used in a bouncing ball example and the results of simulations are presented. The double pendulum system is assumed to be a model of a human arm. The results were compared with 2D approach model of a human arm and also with an experiment. Possibilities of further biomechanics applications are demonstrated using the double pendulum contacting a plain example.

2. The method

2.1. Double pendulum model

The double pendulum is assumed to be composed by two ellipsoids constrained together. Both ellipsoids have semi-principal axes a_{ij}, mass m_i and moments of inertia I_{ij}, $i \in \{1, 2\}$ and $j \in \{1, 2, 3\}$. The global coordinate system $\boldsymbol{x}_1 = [x_1, y_1, z_1]$ is defined to be a Cartesian right handed coordinate system with an origin at frame point of the first pendulum (joint). While $\boldsymbol{x}_2$ and $\boldsymbol{x}_3$ are local coordinate systems of particular bodies with origin located at the centre of the bodies. The two bodies are linked with a spherical kinematic joint together and the first one is linked to a rigid frame also with spherical joint. Whole system of bodies is shown in Fig. 1 and the coordinate systems are displayed.

2.1.1. Spherical joint

A spherical joint is a type of a primitive kinematic constraint with three rotational degrees of freedom.

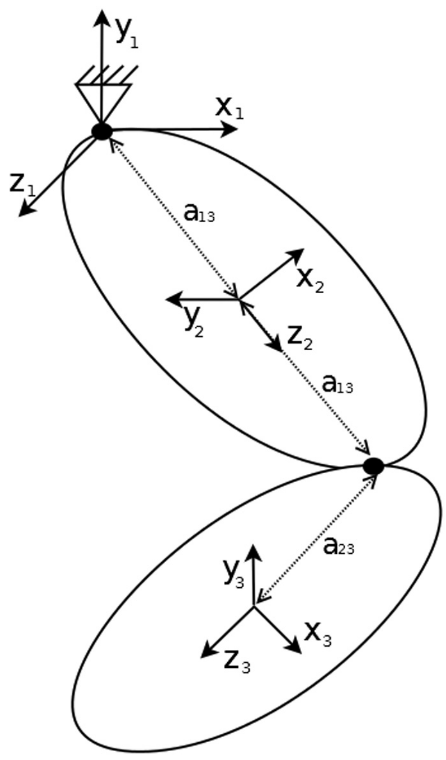

Fig. 1. Double pendulum

Spherical motion can be considered as three independent rotations, namely precession around the z axis represented with angle ψ, nutation around the actual x axis represented with ϑ and rotation around the actual z axis represented by angle φ. The three independent spatial motions can be described by transformation matrices, namely the

$$\boldsymbol{S}_{pre}(\psi) = \begin{bmatrix} \cos(\psi) & -\sin(\psi) & 0 \\ \sin(\psi) & \cos(\psi) & 0 \\ 0 & 0 & 1 \end{bmatrix}, \tag{1}$$

$$\boldsymbol{S}_{nut}(\vartheta) = \begin{bmatrix} 1 & 0 & 0 \\ 0 & \cos(\vartheta) & -\sin(\vartheta) \\ 0 & \sin(\vartheta) & \cos(\vartheta) \end{bmatrix}, \tag{2}$$

$$\boldsymbol{S}_{rot}(\varphi) = \begin{bmatrix} \cos(\varphi) & -\sin(\varphi) & 0 \\ \sin(\varphi) & \cos(\varphi) & 0 \\ 0 & 0 & 1 \end{bmatrix}. \tag{3}$$

Transformation formula in case of a spherical motion can be written using coordinates of centre of gravity and multiplication of precession, nutation and rotation matrices. Thus the general transformation of any point from local to a global coordinate system is described as

$$\boldsymbol{x}_1 = \boldsymbol{x_s} + \boldsymbol{S}_{pre}(\psi)\ \boldsymbol{S}_{nut}(\vartheta)\ \boldsymbol{S}_{rot}(\varphi)\ \boldsymbol{x}_2, \tag{4}$$

where $\boldsymbol{S}_{pre}(\psi)$, $\boldsymbol{S}_{nut}(\vartheta)$ and $\boldsymbol{S}_{rot}(\varphi)$ are transformation matrices of precession, nutation and rotation, respectively. $\boldsymbol{x}_2$ are coordinates of a point at the body expressed in local coordinate system, $\boldsymbol{x_1}$ represents coordinates of this point in the global coordinate system and $\boldsymbol{x}_s$ are coordinates of centre of gravity of body expressed in the global coordinate system. Equation (4) can be rewritten as

$$\boldsymbol{x}_1 = \boldsymbol{x}_{s_i} + \boldsymbol{S}_{1i}(\psi_i, \vartheta_i, \varphi_i)\ \boldsymbol{x}_i, \quad i \in \mathbb{N}, \tag{5}$$

where $\boldsymbol{S}_{1i}$ is a transformation matrix between local body-fixed coordinate system i and global coordinate system 1.

Since the system here considers two bodies, two local body fixed coordinate systems are required, and the global coordinates $\boldsymbol{x}_1$ of any point can be defined:

- The first body global coordinates: $i = 2$

$$\boldsymbol{x}_1 = \boldsymbol{x}_{s_2} + \boldsymbol{S}_{12}(\psi_2, \vartheta_2, \varphi_2)\boldsymbol{x}_2. \tag{6}$$

- The second body global coordinates: $i = 3$

$$\boldsymbol{x}_1 = \boldsymbol{x}_{s_3} + \boldsymbol{S}_{13}(\psi_3, \vartheta_3, \varphi_3)\boldsymbol{x}_3, \tag{7}$$

where $\boldsymbol{x}_{s_2} = [x_{s_2}, y_{s_2}, z_{s_2}]^T$ represents coordinates of centre of gravity of the first body and $\boldsymbol{x}_2$ are coordinates of the particular point in the local coordinate system of the first body. $\boldsymbol{x}_{s_3} = [x_{s_3}, y_{s_3}, z_{s_3}]^T$ are coordinates of centre of gravity of the second body and $\boldsymbol{x}_3$ are coordinates of a point in the local coordinate system of the second body. Variables $\psi_i, \vartheta_i, \varphi_i$, $i \in 2, 3$ are known as Euler's angles [8].

Vector of generalized coordinates of the whole system is defined as

$$\boldsymbol{q} = [x_{s_2}, y_{s_2}, z_{s_2}, \psi_2, \vartheta_2, \varphi_2, x_{s_3}, y_{s_3}, z_{s_3}, \psi_3, \vartheta_3, \varphi_3]^T.$$

The set of kinematics constraint equations can be defined as

$$\boldsymbol{\Phi} = \begin{bmatrix} \boldsymbol{\Phi}_1 \\ \boldsymbol{\Phi}_2 \end{bmatrix} = \begin{bmatrix} \Phi_1 \\ \Phi_2 \\ \Phi_3 \\ \Phi_4 \\ \Phi_5 \\ \Phi_6 \end{bmatrix} = \begin{bmatrix} \boldsymbol{x}_{s2} + \boldsymbol{S}_{12} \begin{bmatrix} 0 \\ 0 \\ -a_{13} \end{bmatrix} \\ \boldsymbol{x}_{s2} + \boldsymbol{S}_{12} \begin{bmatrix} 0 \\ 0 \\ a_{13} \end{bmatrix} - \boldsymbol{x}_{s3} - \boldsymbol{S}_{13} \begin{bmatrix} 0 \\ 0 \\ -a_{23} \end{bmatrix} \end{bmatrix} = \begin{bmatrix} 0 \\ 0 \\ 0 \\ 0 \\ 0 \\ 0 \end{bmatrix}. \tag{8}$$

This generates six equations of the kinematics constraint in term of the local coordinates

$$\boldsymbol{\Phi}(\boldsymbol{q}, t) = \begin{bmatrix} \mathrm{x_{s2}} - \mathrm{a_{13}} \sin(\vartheta_2) \sin(\psi_2) \\ \mathrm{y_{s2}} + \mathrm{a_{13}} \cos(\psi_2) \sin(\vartheta_2) \\ \mathrm{z_{s2}} - \mathrm{a_{13}} \cos(\vartheta_2) \\ \mathrm{x_{s2}} - \mathrm{x_{s3}} + \mathrm{a_{13}} \sin(\vartheta_2) \sin(\psi_2) + \mathrm{a_{23}} \sin(\vartheta_3) \sin(\psi_3) \\ \mathrm{y_{s2}} - \mathrm{y_{s3}} - \mathrm{a_{13}} \cos(\psi_2) \sin(\vartheta_2) - \mathrm{a_{23}} \cos(\psi_3) \sin(\vartheta_3) \\ \mathrm{z_{s2}} - \mathrm{z_{s3}} + \mathrm{a_{13}} \cos(\vartheta_2) + \mathrm{a_{23}} \cos(\vartheta_3) \end{bmatrix} = \boldsymbol{0}, \tag{9}$$

where a_{ij} represent a length of semi-principal axes.

2.2. Equations of motion

Equations of motion are derived using Lagrange equations of second kind with multipliers. Second derivatives on the kinematics constraints were added to the system and these formulate equation of motion of the double pendulum system

$$\begin{bmatrix} \boldsymbol{M} & \Phi_{\mathbf{q}}^T \\ \Phi_{\mathbf{q}} & \boldsymbol{0} \end{bmatrix} \begin{bmatrix} \ddot{\boldsymbol{q}} \\ -\boldsymbol{\lambda} \end{bmatrix} = \begin{bmatrix} \boldsymbol{f}(\boldsymbol{q}, \dot{\boldsymbol{q}}, t) \\ \gamma(\boldsymbol{q}, \dot{\boldsymbol{q}}, t) \end{bmatrix}, \tag{10}$$

where $\boldsymbol{M}$ is mass matrix, $\ddot{\boldsymbol{q}}$ represents generalized accelerations vector, $\boldsymbol{\lambda}$ is vector of Lagrange's multipliers, $\Phi_{\mathbf{q}}$ is the Jacobian of the vector of constraints, $\boldsymbol{f}$ and γ are vectors of external forces (including contact force), and rest after derivation, respectively. Equation (10) is a differential-algebraic equation of second order. An important classification of differential equations is whether it is a stiff or a non-stiff problem, associated with eigenfrequency distribution [4]. The example here is considered to be stiff problem and this can cause difficulties during numerical integration. Thus the special numerical solvers are implemented.

To express accelerations $\ddot{\boldsymbol{q}}$ and solve the equation by numerical integration, the approach called elimination of the Lagrange multipliers is applied. Using this technique, following system is obtained

$$\begin{bmatrix} \dot{\boldsymbol{u}} \\ \dot{\boldsymbol{v}} \end{bmatrix} = \begin{bmatrix} \boldsymbol{v} \\ \ddot{\boldsymbol{q}} \end{bmatrix} = \begin{bmatrix} \dot{\boldsymbol{q}} \\ \boldsymbol{M}^{-1}\{\boldsymbol{f} + \Phi_{\mathbf{q}}^T(\Phi_{\mathbf{q}}\boldsymbol{M}^{-1}\Phi_{\mathbf{q}}^T)^{-1}(\boldsymbol{\gamma} - \Phi_{\mathbf{q}}\boldsymbol{M}^{-1}\boldsymbol{f})\} \end{bmatrix}. \tag{11}$$

Equation (11) can be solved using standard techniques of numerical integration, however it has some undesirable troubles. It might be numerically unstable for a certain properties, thus Baumgarte's stabilization method solving bad stability is applied [4].

This brings new formulation of the first order differential-algebraic equation, which can be numerically solved

$$\begin{bmatrix} \dot{\boldsymbol{u}} \\ \dot{\boldsymbol{v}} \end{bmatrix} = \begin{bmatrix} \boldsymbol{v} \\ \ddot{\boldsymbol{q}} \end{bmatrix} = \begin{bmatrix} \dot{\boldsymbol{q}} \\ \boldsymbol{M}^{-1}\{\boldsymbol{f} + \Phi_{\mathbf{q}}^T(\Phi_{\mathbf{q}}\boldsymbol{M}^{-1}\Phi_{\mathbf{q}}^T)^{-1}(\boldsymbol{\gamma} - 2\alpha\dot{\boldsymbol{\Phi}} - \beta^2\boldsymbol{\Phi} - \Phi_{\mathbf{q}}\boldsymbol{M}^{-1}\boldsymbol{f})\} \end{bmatrix}. \tag{12}$$

Constants α and β were chosen based on literature [4]. MATLAB [6] software is applied to calculate numerical solution. There are some suitable numerical ODE solvers for the stiff problems implemented in MATLAB, such as ODE15s, ODE23t, ODE23tb.

2.3. *Arm gravity motion*

Double pendulum system is used as an approximation of a human arm. Valdmanová in [13] established a 2D model of an arm based on multibody approach. This model represents the main parts of a human arm, namely the upper arm, the forearm and the hand. Later on, the model is simplified into a two bodies system only, since the motion between forearm and hand can be neglected. Valdmanová compared in her work a simulation with a result of an experiment. Joints between bodies are modelled to be joints with an internal stiffness. Thus the bodies load with torques representing rigidity of a shoulder and of an elbow, respectively. Geometric properties of the bodies are set of from [13]. Passive bending moments of joints are defined by curves based on [9].

Initial position of the arm corresponding to an experiment is based on anthropometric data, namely the driver's position while holding a steering wheel. Initial conditions of the arm are shown in Fig. 2, where angles $\varphi_1 = -45°$ and $\varphi_2 = 23°$.

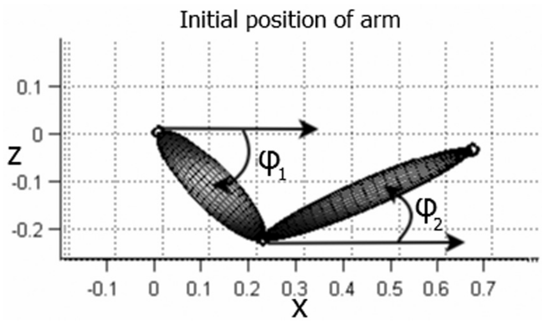

Fig. 2. Initial position of arm

2.4. *Contact calculation*

This work concerns possible impact between any ellipsoid of the double pendulum and a plain. If the bodies get into a collision, the crucial question is to evaluate impact performance of a contact force. Several approaches for a contact force expression were developed. The concept of this work is to use a continuous contact force model, where the contact force is a function of local penetration δ and local penetration velocity $\dot{\delta}$, respectively. Three contact force models are presented here, namely Hertz model, spring-dashpot model and non-linear damping model, respectively. To capture the effect of contact force in case of interaction bodies, the penetration depth is calculated. To identify whether the bodies are getting into a collision, the minimum distance between them is required. As long as the distance is positive, the bodies are disjointed. Change of the sign indicates a collision and negative distance magnitude is equal to penetration δ. Several algorithms for minimum distance calculation were published [1,3,11,14]. This study is focused on the analytical approach of minimum distance problem [2]. Idea of this method is to create a new plain, parallel to an initial one and tangential to the ellipsoid. When the common point, marked as C, of a new plain and of an ellipsoid is detected, distance between this point and the plain can be calculated, using adequate equation from analytical geometry. There always exist two such parallel plains, as is shown in Fig. 3.

2.5. *Minimum distance problem application*

Let us show analytical solution of the contact problem between an ellipsoid and a plain. The standard equation of an ellipsoid centred at the origin of a Cartesian coordinate system and

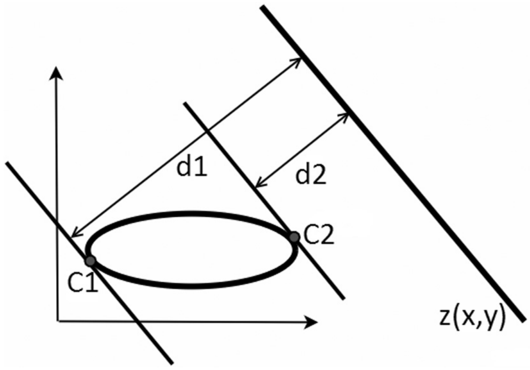

Fig. 3. Ellipsoid and two parallel plains

aligned with the axes is

$$\frac{x^2}{a^2} + \frac{y^2}{b^2} + \frac{z^2}{c^2} = 1, \tag{13}$$

where a, b and c are constants, which represent the length of semi-principal axes. Equation (13) can be rearranged by set of substitutions to the form

$$Ax^2 + By^2 + Cz^2 + D = 0. \tag{14}$$

A general equation of plain can be defined as

$$kx + ly + mz + n = 0. \tag{15}$$

An ellipsoid is a type of a quadric surface in coordinates $\{x, y, z\}$. Thus equation (15) can be rearranged to be a function $z = z(x, y)$ as

$$z(x, y) = -\frac{k}{m}\,x - \frac{l}{m}\,y - \frac{n}{m}. \tag{16}$$

A plain can be defined using one point and two vectors. To ensure new plain being parallel with the initial one, at least two gradient vectors of both plains have to be the same. The two gradient vectors together with one point on the surface of the ellipsoid, can identify the required tangential plain. Hence the gradients $\frac{\partial z}{\partial x}$ and $\frac{\partial z}{\partial y}$ of the plain $z = z(x, y)$ are evaluated as

$$\frac{\partial z(x, y)}{\partial x} = -\frac{k}{m} \tag{17}$$

and

$$\frac{\partial z(x, y)}{\partial y} = -\frac{l}{m}. \tag{18}$$

Equation (14) is differentiated with respect to variables x and y as

$$\frac{\partial}{\partial x}: \qquad 2Ax + 2By \underbrace{\frac{\partial y}{\partial x}}_{0} + 2Cz \underbrace{\frac{\partial z}{\partial x}}_{-\frac{k}{m}} = 0 \tag{19}$$

and

$$\frac{\partial}{\partial y}: \qquad 2Ax \underbrace{\frac{\partial x}{\partial y}}_{0} + 2By + 2Cz \underbrace{\frac{\partial z}{\partial y}}_{-\frac{l}{m}} = 0. \tag{20}$$

Since x and y are independent variables, mixed derivatives are equal to zero. If equation (17) and equation (18) are substituted into equation (19) and equation (20) together with general equation of ellipsoid (14) generate the system of three equations for unknown variables x, y and z as

$$2Ax - 2Cz\,\frac{k}{m} = 0, \tag{21}$$

$$2By - 2Cz\,\frac{l}{m} = 0 \tag{22}$$

and

$$f(x, y, z) = Ax^2 + By^2 + Cz^2 + D = 0. \tag{23}$$

Solution of this system of equations generates two points, namely point $C_1 = [x_{10}, y_{10}, z_{10}]$ and point $C_2 = [x_{20}, y_{20}, z_{20}]$, which are mutual points of the body and the new tangential plain. These points are also the points of extrema distance (minimum and maximum) between plain and body, see Fig. 3. When coordinates of these points are known, it is very straightforward to calculate distance between these points and plain. The distance between point $X_0 = [x_0, y_0, z_0]$ and plain $kx + ly + mz + n = 0$ is given by

$$d = \frac{kx_0 + ly_0 + mz_0 + n}{\sqrt{k^2 + l^2 + m^2}}. \tag{24}$$

Equation (24) results two extrema distances between the ellipsoid and the plain, so minimum one is required. However, this method is working only for the ellipsoid, whose semi principal axes are parallel with coordinate axes. Both of the entities (the body and the plain) have to be expressed in the identical coordinate system to applied the method defined above. Here, the equation of the plain in form (15) is expressed in the global, frame-fixed, coordinate system, but equation of ellipsoid (13) is evaluated in the local body fixed coordinate system.

2.5.1. Transformation

Actual position of any point of ellipsoid is defined by 6 independent coordinates x_s, y_s, z_s, ψ, ϑ, φ, where x_s, y_s and z_s are coordinates of centre of gravity and ψ, ϑ and φ are Euler's angles. The principle applied here is based on the transformation of a plain equation from a global coordinate system, marked as $\boldsymbol{x}_1$ into a local body fixed coordinate system, marked as $\boldsymbol{x}_2$. For the transformation, it is useful to write the plain and the ellipsoid equations in a matrix form using homogeneous coordinates. Thus the plain equation is

$$\begin{bmatrix} k & l & m & n \end{bmatrix} \begin{bmatrix} x_1 \\ y_1 \\ z_1 \\ 1 \end{bmatrix} = 0, \tag{25}$$

or in compact matrix form

$$\boldsymbol{r}^T \boldsymbol{x}_1 = 0. \tag{26}$$

The ellipsoid equation comes to

$$\begin{bmatrix} x_2 & y_2 & z_2 & 1 \end{bmatrix} \begin{bmatrix} A & 0 & 0 & 0 \\ 0 & B & 0 & 0 \\ 0 & 0 & C & 0 \\ 0 & 0 & 0 & D \end{bmatrix} \begin{bmatrix} x_2 \\ y_2 \\ z_2 \\ 1 \end{bmatrix} = 0, \tag{27}$$

or in matrix form

$$(\boldsymbol{x}_2)^T \boldsymbol{A} \boldsymbol{x}_2 = 0. \tag{28}$$

As is mentioned above, both the entities need to be expressed in the same coordinate system. The very crucial question is how to transform those equations to be expressed in the same coordinate system. A purpose of the transformation is to obtain equations in such a form, which the method of minimum distance calculation can be applied on. There are two possibilities how to assure this condition:

- The first option is using matrix $\boldsymbol{T}$ to transform ellipsoid equation (28) from the local coordinate system to the global one (where the plain is defined) as

$$\boldsymbol{x}_1^T \boldsymbol{T}^T \boldsymbol{A} \boldsymbol{T} \boldsymbol{x}_1 = 0. \tag{29}$$

- The second one is to use matrix $\boldsymbol{T^{-1}}$ to transform plain equation (26) from the global coordinate system to the local one (where the ellipsoid is defined) as

$$\boldsymbol{r} \boldsymbol{T}^{-1} \boldsymbol{x}_2 = 0, \tag{30}$$

  in which $\boldsymbol{T}$ is a transformation matrix between the local and the global coordinate system and obviously $\boldsymbol{T}^{-1}$ is a transformation matrix from the global to the local coordinate system.

- The first option results a scalar equation, but it is highly non-linear and it is not possible to arrange that in a form

$$\tilde{A}x_1^2 + \tilde{B}y_1^2 + \tilde{C}z_1^2 + \tilde{D} = 0, \tag{31}$$

  where $\tilde{A}$, $\tilde{B}$, $\tilde{C}$ and $\tilde{D}$ can be any arbitrary constants. So, this option is not suitable for this purpose.

- The second option also results a scalar equation, but this can be written in the same form as the original one as

$$\tilde{k}x_2 + \tilde{l}y_2 + \tilde{m}z_2 + \tilde{n} = 0, \tag{32}$$

  where $\tilde{k}$, $\tilde{l}$, $\tilde{m}$, $\tilde{n}$ are constants defined by particular transformations.

Now both (the plain and the ellipsoid) equations are expressed in the same coordinate system (local body-fixed) and the standard distance calculation method described above can be used.

Equation of a transformed plain equation (32) together with original equation of ellipsoid (14) are satisfactory inputs to the minimum distance calculation method. By solving system of equations, two points of extreme distance C_1 and C_2 are evaluated and two extreme distances can be calculated and obviously minimum one is required

$$d = \min_i(d_i) = \frac{\tilde{k}x_{i0} + \tilde{l}y_{i0} + \tilde{m}z_{i0} + \tilde{n}}{\sqrt{\tilde{k}^2 + \tilde{l}^2 + \tilde{m}^2}}, \qquad i \in \{1, 2\}. \tag{33}$$

2.6. Contact force

This study is focused on a continuous models implementation, in which impact force is defined to be a function of local penetration δ and local penetration velocity $\dot{\delta}$, respectively. Relative normal contact force acts at the contact point and can be defined as

$$\boldsymbol{f}_n = \boldsymbol{f}_n(\delta, \dot{\delta}). \tag{34}$$

Normal vector of the ellipsoid expressed at point C is then

$$^{\boldsymbol{c}}\tilde{\boldsymbol{n}} = \left[\left.\frac{\partial f(x,y,z)}{\partial x}\right|_C, \left.\frac{\partial f(x,y,z)}{\partial y}\right|_C, \left.\frac{\partial f(x,y,z)}{\partial z}\right|_C \right]^T, \tag{35}$$

where f is the smooth regular surface, defined by (23). For the purpose of defining contact force, normal vector is normalized to have a unit length

$$^{c}\boldsymbol{n} = \frac{^{\boldsymbol{c}}\tilde{\boldsymbol{n}}}{\|^{c}\,\tilde{\boldsymbol{n}}\,\|}. \tag{36}$$

Calculation of the relative normal contact velocity (penetration velocity) is done by differentiating equation (24)

$$\dot{\delta} = \frac{\mathrm{d}}{\mathrm{d}t}\delta = \frac{\mathrm{d}}{\mathrm{d}t}\left\{ \frac{kx_0 + ly_0 + mz_0 + n}{\sqrt{k^2 + l^2 + m^2}} \right\}. \tag{37}$$

Vector of contact force $\boldsymbol{f}_n$ can be evaluated using entities above, regarding adequate contact force models:

- Hertz model
$$\boldsymbol{f}_n = f_n\, ^{\boldsymbol{c}}\boldsymbol{n} = k_h\, \delta^n\, ^{\boldsymbol{c}}\boldsymbol{n}. \tag{38}$$

- Spring dashpot model
$$\boldsymbol{f}_n = f_n\, ^{\boldsymbol{c}}\boldsymbol{n} = (k_{sd}\, \delta + b_{sd}\, \dot{\delta})^{\boldsymbol{c}}\boldsymbol{n}. \tag{39}$$

- Non-linear damping model

$$\boldsymbol{f}_n = f_n\, ^{\boldsymbol{c}}\boldsymbol{n} = (k_{nl}\, \delta^n + b_{nl}\, \delta^p \dot{\delta}^q)^{\boldsymbol{c}}\boldsymbol{n}. \tag{40}$$

Parameters k, b, p, q, n are constants and it is common to set them $p = n$ and $q = 1$. Parameter k represents artificial spring stiffness and b is artificial damping coefficient. Constants k and b depend on various aspects, such as material and geometric properties of contacting bodies. Acting force $\boldsymbol{f}_n$ is then translated to the centre of gravity of the body including a torque $\boldsymbol{m}$ caused by the translation. Fig. 4 shows two equivalent systems, first one with contact force acting at the contact point and second system loaded with moment and force acting at the centre of gravity.

Moment is then defined as

$$\boldsymbol{m} = \boldsymbol{r} \times \boldsymbol{f}_n, \tag{41}$$

where vector $\boldsymbol{r}$ can be expressed using coordinates of a contact point.

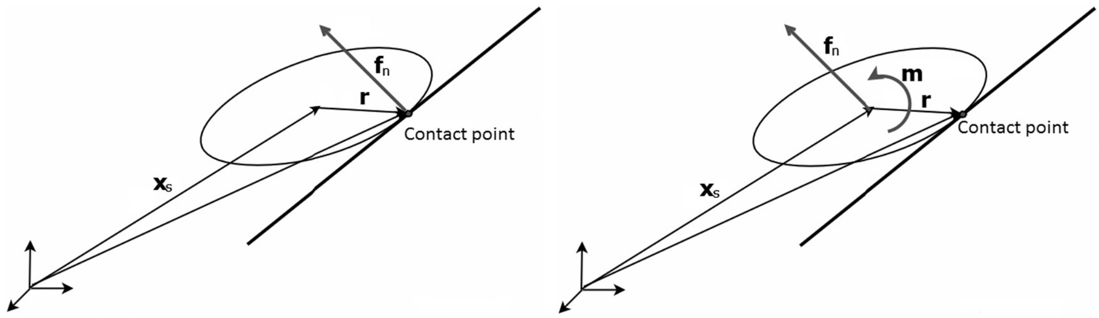

(a) Original position of contact force (b) Translated force and a moment

Fig. 4. Two equivalent systems

2.6.1. *Force implementation*

In case of contacting bodies right hand side of equation of motion (10) includes contact force $\boldsymbol{f}_n$ and torque $\boldsymbol{m}$ and comes to a following form

$$\boldsymbol{f} = \begin{bmatrix} F_{nx} \\ F_{ny} \\ F_{nz} - mg \\ M_x \\ M_y \\ M_z \end{bmatrix}. \tag{42}$$

For separated bodies, $\boldsymbol{f}_n = \mathbf{0}$ and thus vector $\boldsymbol{f}$ comes to a simple form of unconstrained model loaded only with gravity

$$\boldsymbol{f} = \begin{bmatrix} 0 \\ 0 \\ -mg \\ 0 \\ 0 \\ 0 \end{bmatrix}. \tag{43}$$

2.7. *Contact parameters optimization*

Continuous model defines contact force to be a function of penetration δ between contacting bodies and penetration velocity $\dot{\delta}$ and parameters k and b, respectively. Experimental results of simple impact example are used in comparison with numerical simulations to obtain appropriate values of parameters k and b for each model. By varying the theoretical quantities, the most corresponding results of simulation to an original experiment can be achieved. Stiffness and damping parameters are so called optimization parameters and difference between experimental and calculated results is an objective function, which is desirable to be minimised. Th method of numerical optimization is introduced here. An example of application considered here is bouncing ball, published in [5]. An elastic ball with an initial height equalling to 1.0 m, mass of 1 kg, moment of inertia equalling to $0.1\ \mathrm{kg} \cdot \mathrm{m}^2$ and radius equalling to 0.1 m, are released from initial position under action only with acceleration of gravity g equalling to $9.81\ \mathrm{m} \cdot \mathrm{s}^{-2}$, see Fig. 5. The ball is falling down until it collides with a rigid ground. When the ball collides a contact takes place and the ball rebounds, producing a jump, which height depends on parameters of the contact force.

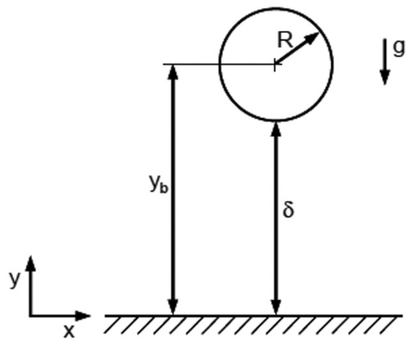

Fig. 5. Bouncing ball example [5]

MATLAB software is used to solve the equation of motion of the ball and software optiSLang 3.2.0, controls variation of input parameters k and b, respectively. MATLAB software version R2011b under MS Windows platform on single processor Core Duo T2400 computer with frequency of 1.83 GHz a 2 MB L2 cache, is used to numerically solve example of bouncing ball. MATLAB has implemented several numerical solvers for these stiff problems. However, it is not very straightforward to select a suitable one. In order to choose the best one for further applications, based on minimum calculation time, four stiff numerical solvers ODE are applied on the same system. Simulations of bouncing ball example with 1 s and 5 s duration time are presented.

3. Results

3.1. Arm gravity motion

Following Fig. 6a shows the motion of the elbow of the right arm. While solid curve represents 3D double pendulum simulation, dash-dot curve represents 2D simulation of arm model [13] and the points represent experimental results [13]. The second graph, see Fig. 6b, shows motion of the wrist, where curves are same with the Fig. 6a.

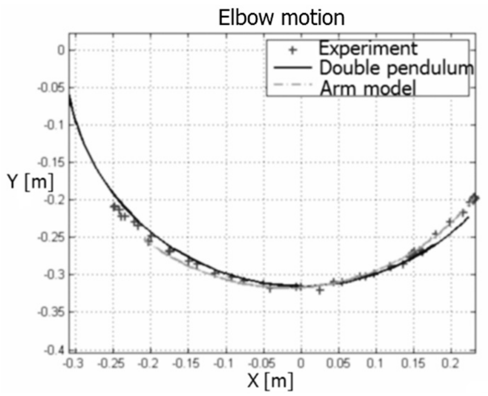

(a) Trajectories of an elbow

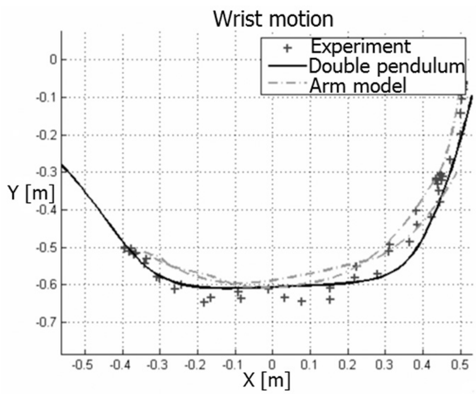

(b) Trajectories of a wrist

Fig. 6. Comparison of human arm models and experiment

Previous figures show the results of simulations in comparison with experiment. Although the trajectory of the wrist slightly differs from the experiment and also from Valdmanova's simulation, the results refer to an equivalence of the systems.

3.2. Solver selection

The most suitable numerical solver for this particular problem are chosen based on computation time of four different stiff solvers. These are applied on the same system, namely the bouncing ball example. Simulation of 1 s and 5 s duration time are tested and computation times are compared.

Table 1 shows the computation times of particular simulations. Based on the results, solver ODE15s is used in MATLAB for the numerical integration in the further calculations.

Table 1. Calculation time of identical simulation with different solvers

Solver	Computation time [s] 1 s simulation	5 s simulation
ODE23t	169	1 820
ODE23tb	278	2 675
ODE15s	166	1 382
ODE23s	1 592	20 045

3.3. Numerical optimization of contact parameters

Solver ODE15s implemented in MATLAB software is used to solve the equation of motion of a bouncing ball. Software optiSLang controls variation of contact parameters k and b, respectively, to reach the most corresponding results of simulation to an original experiment. Mathematics optimization principle is applied on the three contact force models. Namely Hertz model, spring-dashpot model and non-linear damping model, respectively. Calculated position of ball centre of gravity together with the initial experiment are shown in following Fig. 7.

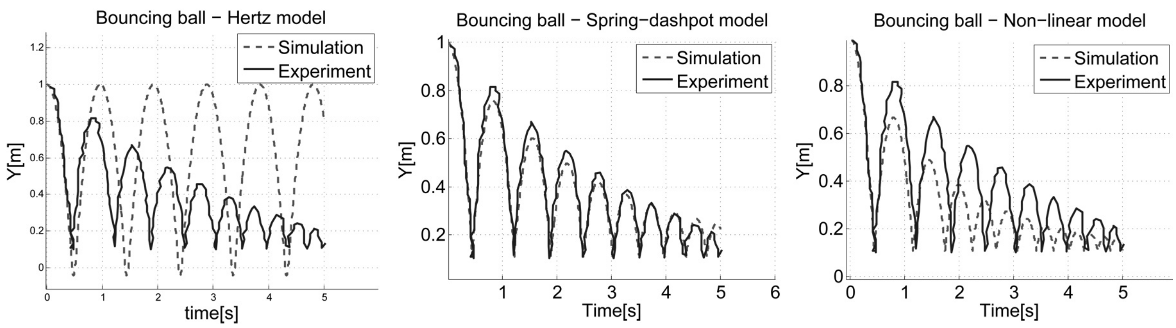

(a) Hertz model (b) Spring-dashpot model (c) Non-linear damping model

Fig. 7. Numerical optimizations results applied on bouncing ball example

Evaluated contact force parameters are displayed in Table 2.

Table 2. Contact parameters of particular force models

Model / Parameter	k	b
Hertz's	10 000	–
Spring-dashpot	3.303e+7	2.157e+4
Non-linear damping	3.009e+7	3.000e+4

3.3.1. Discussion

The Hertz model performs an elementary model suitable for the first approximation of impact. Since it does not take energy dissipation phenomena into account, it is not applicable for all configurations. In case of a fully elastic impact this model can provide satisfactory results. The spring-dashpot model takes energy dissipation effect into account, through damping coefficient that includes a coefficient of restitution. It refers to a more realistic situation, since it is not limited with an elastic impact. By varying with the coefficient of restitution between 0 and 1, phenomena between a fully plastic and a fully elastic impact can be captured. The non-linear damping force model also works with dissipation of energy, but the calculation states unstable. Compared to the spring-dashpot model, the curves of an experiment and a numerical simulation differ significantly. Based on the calculations, the spring-dashpot model provides results the most corresponding with the experiment. Due to this fact, it is used in further applications.

3.4. Double pendulum contacting a plain

The double pendulum system was described and validated to be a suitable approximation of a human arm. Purpose of this part is to evaluate results of the system including a contact with a plain. This can be applied in further applications such as the approximation of an arm or a leg undergoing into an impact with an infrastructure. Motion of the double pendulum that getting into a contact with plain is displayed in Fig. 8.

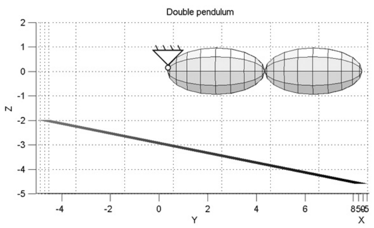

(a) $t = 0$ s

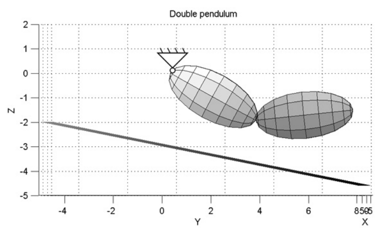

(b) $t = 0.25$ s

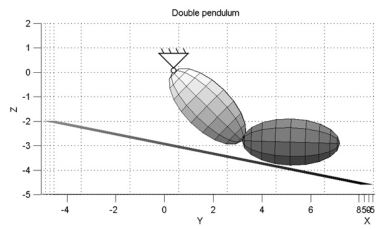

(c) $t = 0.5$ s

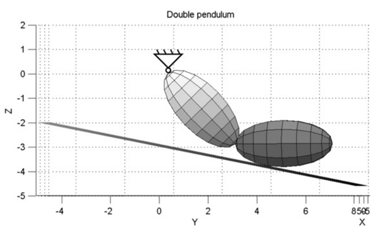

(d) $t = 0.75$ s

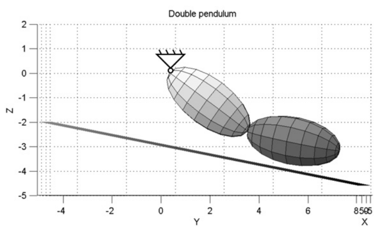

(e) $t = 1$ s

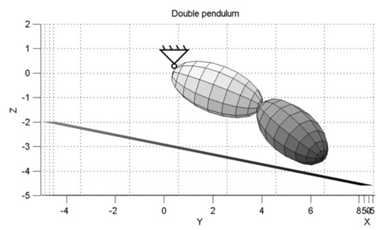

(f) $t = 1.25$ s

Fig. 8. Position of the double pendulum contacting a plain

4. Conclusion

Contact or impact scenario in virtual human body modelling plays significant role in biomechanics research. Various approaches in biomechanical modelling are currently developed The purpose of this work is to evaluate and test the algorithm for the double pendulum getting into a contact with a plain. The equations of motion of the double pendulum were derived using the Lagrange equation of second kind with multipliers. Evaluating of contact force parameters is performed using numerical optimization principle applied on bouncing ball example. Three contact force models are investigated, namely the Hertz model, the spring-dashpot model and the non-linear damping model. Optimized contact force parameters are used in the double pendulum impact scenario. Assuming a reference of biomechanics researches, the double pendulum system might approximate various segments of a human body. Application of a human arm problem was verified here. Impact scenario is demonstrated on the double pendulum getting into a contact with plain.

Acknowledgements

This work is supported by internal grant project SGS-2013-026.

References

[1] Boss, M., McPhee, J., Volumetric contact dynamics model and experimental validation of normal forces for simple geometries, Proceedings of the ASME 2011 International Design Engineering Technical Conferences & Computers and Information in Engineering Conference IDETC/CIE 2011, 2011.

[2] Drexel University. The Math forum @ Drexel 2010.

[3] Eberly, D., Intersection of ellipsoids, Geometric tools, LLC, 2010.

[4] Hajžman, M., Polach, P., Application of stabilization techniques in the dynamic analysis of multibody systems, Applied and Computational Mechanics 1 (2) (2007) 479–488.

[5] Machado, M. F., Flores, P., A novel continuous contact force model for multibody dynamics, Proceedings of the ASME 2011 International Design Engineering Technical Conferences & Computers and Information in Engineering Conference IDETC/CIE 2011, 2011.

[6] MathWorks. MATLAB R2010a.

[7] Moser, A., Steffan, H., Kasanický, G., The pedestrians model in PC-Crash-Introduction of a multibody system and its validation. SAE The engineering society for advancing mobility land sea air and space, 1999.

[8] Pfeiffer, F., Unilateral multibody dynamics, Meccanica 34 (1999) 437–451.

[9] Robbins, D. H., Anthropometry of motor vehicle occupants, Technical report, The University of Michigan, Transportation Research Institute, 1983.

[10] Shabana, A. A., Dynamics of multibody systems. 3rd edition, Cambridge University Press, Cambridge, 2005.

[11] Sohn, K. A., Juttler, B., Kim, M. S., Wang, W., Computing distance between surfaces using line geometry, IEEE Computer society, 2002.

[12] Stejskal, V., Valášek, M., Kinematics and dynamics in machinery, Marcel Dekker, New York, 1996.

[13] Valdmanová, L., Multibody model of upper extremity in 2D, Master thesis, University of West Bohemia, Pilsen, 2009. (in Czech)

[14] Wang, W., Choi, Y. K., Chan, B., Kim, M. S., Wang, J., Efficient collision detection for moving ellipsoids using separating planes. Computing 72 (2004) 235–246.

[15] Zhou, Q., Quade, M., Du, H., Concept design of a 4-DOF pedestrians legform. ESV Technical paper 07-0196, 2007.